

Water Resources Research

RESEARCH ARTICLE

10.1029/2018WR023477

Key Points:

- Precipitation, runoff, evapotranspiration, soil moisture, and root zone drainage are quantified over 13 years at a semiarid savanna site
- Evapotranspiration dominates water loss from the root zone, runoff is small, and deep drainage is minuscule
- Carryover of soil moisture from summer rainfall to the following spring challenges assumptions about dryland soil water residence times

Supporting Information:

- Supporting Information S1

Correspondence to:

R. L. Scott,
russ.scott@ars.usda.gov

Citation:

Scott, R. L., & Biederman, J. A. (2019). Critical zone water balance over 13 years in a semiarid savanna. *Water Resources Research*, 55, 574–588. <https://doi.org/10.1029/2018WR023477>

Received 11 JUN 2018

Accepted 5 DEC 2018

Accepted article online 17 DEC 2018

Published online 24 JAN 2019

Published 2018. This article is a U.S. Government work and is in the public domain in the USA.

Critical Zone Water Balance Over 13 Years in a Semiarid Savanna

Russell L. Scott¹  and Joel A. Biederman¹ 

¹Southwest Watershed Research Center, USDA Agricultural Research Service, Tucson, AZ, USA

Abstract Quantifying how much and when precipitation (P) becomes runoff (R), evapotranspiration (ET), and drainage from the root zone (D) is key to understanding how climate and land use impact hydrology of the critical zone. We quantify water balance dynamics of a semiarid savanna with a summer/winter rainfall pattern with 13 years of water fluxes and soil moisture. We find multiyear P is partitioned 96% to ET and 7% to R, while D (−3%) is negligible when considering measurement uncertainty. While weather regulates ET over diurnal time scales, soil water inputs control seasonal to annual ET amounts. Seasonal water availability, estimated by soil moisture inputs, is more closely tracked by ET rather than time-averaged soil moisture or P. Surprisingly, we find significant, episodic carryover of soil moisture from the summer to spring growing season. Abundant late-summer P can supply ET in the subsequent spring, even after multimonth dry periods. However, over an annual cycle beginning in early summer, nearly all soil moisture is used by ET. Likewise, D beyond the monitored root zone, assisted by downward hydraulic distribution in plant roots, occurs within a season, but this is counteracted by subsequent ET extraction of deep moisture over the year. Thus, negligible long-term D occurs, though there is considerable uncertainty in estimation of this small flux as the residual of much larger ones. These comprehensive, long-term measurements support expectations about the overriding importance of ET in the dryland critical zone water balance and reveal an unexpected degree of interseasonal water storage.

Plain Language Summary One of the most enduring and important questions for hydrology is how water input in the form of precipitation is partitioned among evapotranspiration, runoff, groundwater recharge, and storage of moisture in the soil. We quantified how precipitation was partitioned at a semiarid savanna site in Arizona, USA, with 13 years of data. We found that almost all of the precipitation goes into evapotranspiration with only a small of runoff and negligible recharge. Contrary to expectations, we saw significant, episodic carryover of soil moisture from the summer/fall growing season to the subsequent springtime when the plants awake from winter dormancy and extract the stored moisture. These comprehensive, long-term measurements support expectations about the overriding importance of ET in semiarid watersheds' water balance and reveal a surprising degree of interseasonal water storage.

1. Introduction

The critical zone is the near-surface environment where rock, soil, water, air and life interact (Brooks et al., 2015). In this zone, one of the most enduring and important questions for hydrology is how water input (i.e., precipitation, P) is partitioned among evapotranspiration (ET), runoff (R), drainage below the root zone (D), groundwater recharge, and soil moisture (SM) storage. This hydrologic partitioning links the water cycle with the many other energy and mass cycles and transformations occurring in the critical zone (Rodríguez-Iturbe, 2000). Because of inherently high temporal variability in P and its partitioning, there is an acute need for continuous, multiyear measurements of hydrologic states and fluxes (Newman et al., 2006). This is especially true in dryland environments, where P is highly variable in both time and space (Nicholson, 2011; Noy-Meir, 1973).

The critical zone extends from the top of the canopy to the groundwater table, but the partitioning of P occurs within the canopy and the root zone. The water balance equation of this zone (depicted in Figure 1) is as follows:

$$Zd\theta/dt = P - ET - R - D \quad (1)$$

where θ is volumetric SM state, and the fluxes P, ET, and R are defined above. Here we define the flux D as drainage from the root zone at depth Z, the maximum depth to which the moisture status of the root zone is

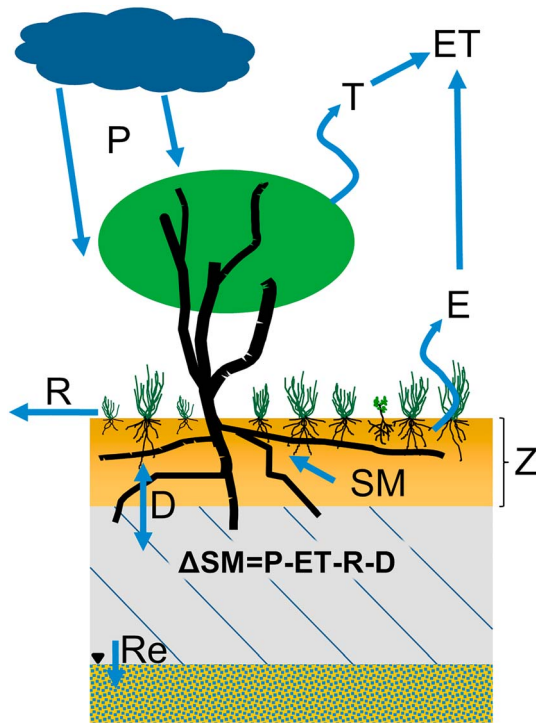


Figure 1. Critical zone water balance where the change in depth-integrated root zone soil moisture ($\Delta SM = Zd\theta/dt$) is balanced by precipitation (P) minus surface runoff (R), evapotranspiration (ET), and drainage (D) below the maximum measurement depth (Z). Hatched region indicates unsaturated zone below the bulk of the root zone and typically not monitored by soil moisture (SM) sensors. Recharge (Re) is D permanently lost beyond the root zone that crosses the water table.

monitored. Recharge is the drainage flux beyond the root zone that becomes groundwater. Recharge is often estimated by long-term D in cases where there is negligible flux divergence between the bottom of the root zone and the water table. Ideally, Z exceeds the depth of all plant roots, but, in practice, this is difficult to guarantee. Especially in natural systems, some roots may extend below the depth to which SM probes are installed to quantify θ . Therefore, our definition of D includes the possibility that water below the depth Z may be accessible by the deep roots of plants to support their transpiration. D, calculated from the water balance equation, can at times be positive or negative. Downward drainage ($D > 0$) out of the monitored root zone can be due to physical infiltration beyond depth Z or may also occur due to biologically mediated water movement from shallow to deep plant roots, termed downward hydraulic redistribution (HR) or hydraulic descent (Burgess et al., 1998; Caldwell et al., 1998; Hultine et al., 2004). Upward drainage ($D < 0$) can be due to plant soil water uptake below depth Z that either goes toward transpiration or is deposited at shallower depths, called upward HR or hydraulic lift. Indeed, HR occurs in many plant types (Nadezhkina et al., 2010) including the desert trees in this study (Barron-Gafford et al., 2017; Scott et al., 2008).

In this paper, we examine a 13-year data set of all the terms in equation (1) collected at subdaily intervals for a semiarid savanna located in southwest United States. Our main objective is to quantify and characterize the components of the critical zone water balance over seasonal to interannual time scales. Water balance characterization is needed to address important hydrological questions including the following: (1) How much rainfall becomes flash floods? (2) How much P becomes available for plant productivity? (3) When, where, and how much is groundwater recharged? And (4) how do changes in land cover impact hydrologic partitioning?

This region of the world is characterized by a bimodal (summer/winter)

annual P distribution with rainfall occurring mainly during hot summers and cool winters separated by fall and late spring periods with very little rainfall. The water balance at this site is representative of the region's shrublands and grasslands with varying amounts of woody plants (trees and shrubs), grasses, and bare soil (Biederman et al., 2017; Scott, 2010).

Previous research has identified many salient features of water balance dynamics in the drylands of the American Southwest. In summer, P is often highly variable in space and concentrated in time, with its dominant origin being convective thunderstorms associated with the North American monsoon (Adams & Comrie, 1997). In winter, P is usually much more widespread and of lower intensity due to the frontal origin of storms. Most of the R occurs as flash floods during summer, when P intensity exceeds the infiltration capacity of the land surface (Goodrich et al., 2004). On small watershed scales of a few hectares or less, R, on a per-unit-area basis, can range from 3% to 14% of P (Polyakov et al., 2010), and it decreases with increasing watershed area due to channel infiltration losses (Goodrich et al., 1997). Perennial streams in this region, though uncommon, occur where the groundwater table intersects the land surface. However, like the present study site, most of the land surface or "upland" is far above the water table, making groundwater inaccessible to plants. Groundwater is recharged primarily along mountain fronts (Ajami et al., 2011; Wilson & Guan, 2004) with a smaller amount occurring due to infiltration losses in large channels (Goodrich et al., 2004; Pool, 2005), although recent results suggest a possible contribution by infiltration in small channels (Schreiner-McGraw & Vivoni, 2017). Chloride borehole measurements and modeling have shown there is likely very little recharge occurring under the nonmountainous upland regions (Coes & Pool, 2007; Scanlon et al., 1999, 2006; Walvoord et al., 2002). Opportunistic dryland vegetation exerts a strong control on SM and typically captures all infiltration before it can move beyond the root zone (Andraski, 1997; Collins & Bras, 2007; Sandvig & Phillips, 2006; Scanlon et al., 2005; Seyfried et al., 2005).

In the Southwest, atmospheric evaporative demand nearly always exceeds the supply of moisture in the critical zone. Thus, ET is a large component of the water balance and is closely tied with P inputs (Biederman et al., 2016). Studies throughout the region have indicated close coupling between shallow SM and ET (Kurc & Small, 2004; Vivoni et al., 2008). When significant rains ($> \sim 2.5$ mm,) fall in summer, dryland plants quickly upregulate, photosynthesize, and transpire (Huxman et al., 2004; Reynolds et al., 2004), but SM supply usually limits ET, even in the wettest summer rainy seasons (Kurc & Small, 2004; Novick et al., 2016). Recent results employing ET and carbon dioxide flux measurements from diverse dryland ecosystems have shown that annual plant photosynthesis is more strongly predicted by ET than by P (Biederman et al., 2016). Biederman et al. (2018) hypothesize that this is because over seasonal to annual time scales ET quantifies the amount of P partitioned to recharge SM, and ET reflects when SM becomes available to drive ecosystem carbon cycling processes.

With low and intermittent rainfall, dryland regions are expected to have dynamic SM only in shallow soil layers with most of the infiltration/ET confined within the upper root zone ($< \sim 30$ -cm depth). Infiltration depths and SM storage are limited in summer due to the high evaporative demand and opportunistic vegetation (Kurc & Small, 2007; Seyfried et al., 2005). However, when plant activity is downregulated in winter due to colder, occasionally freezing temperatures, more substantial infiltration and buildup of SM storage can occur (Kurc & Small, 2007; Petrie et al., 2015; Scanlon et al., 2005; Scott et al., 2000). Significant SM storage in winter can fuel a typically shorter and more ephemeral spring growing season as seasonal rainfall totals are smaller and more variable in winter than in summer (Biederman et al., 2018; Petrie et al., 2015; Scott et al., 2010). SM storage is typically exhausted twice annually, during the dry early summer following the spring growing season and the dry late fall after the summer monsoon growing season (Kurc & Small, 2007; Scott et al., 2009, 2010). For this reason, hydrologists have typically defined the start of a *water year*, the time when transpiration by plants will have largely ceased and the change in yearly SM storage is minimal (Dingman, 2002), to be 1 October or 1 November for the western United States.

Many of the above expectations for dryland critical zone water balance come from studies lasting at most several years. This may severely limit our understanding, as the interannual variability of P can exceed 50% of mean annual P (Biederman et al., 2017) and hydrologically significant events occur rarely in these arid regions (Knapp et al., 2015). The 13-year record presented here enables us to draw more robust conclusions that account for the interannual variability of P and the other water balance terms for an upland savanna site. Here we test the following expectations about the critical zone water balance in drylands: (1) Soils are infrequently wetted beyond shallow root zone depths ($< \sim 30$ cm). Deeper, more persistent wetting occurs episodically and mainly in winter when plant activity is limited and evaporative demand is low. (2) Seasonal water availability, estimated by SM inputs, is best quantified by ET rather than the commonly used, time-averaged SM or P. (3) Precipitation stored as SM is reliably depleted within the current (i.e., spring or summer) growing season. Therefore, seasonal ET should be constrained by within-season SM inputs. (4) Long-term D is expected to be near zero, resulting in negligible groundwater recharge.

2. Site Description

Data from 2004 through 2016 for this study come from the Santa Rita Mesquite Savanna (Scott et al., 2009; AmeriFlux site US-SRM, 31.8218°N, 110.8668°W, elevation: 1,116 m) located in the Santa Rita Experimental Rangeland (McClaran, 2003). The site has a mix of low-stature trees/shrubs, grasses, and succulents and is classified as a woody savanna. The tree cover fraction, consisting mainly of velvet mesquite (*Prosopis velutina*), is 30–35%. Perennial bunchgrass (*Eragrostis lehmanniana*, *Digitaria californica*, *Muhlenbergia porteri*, *Bouteloua eriopoda*, and *Aristida* spp.) cover is around 15–25%, and scattered subshrubs and succulents cover fractions are low. The remaining bare soil (40–50%) supports annual grasses and forbs when rainfall is sufficient. Soils are deep loamy sands (coarse-loamy, mixed, superactive, nonacid, and thermic Ustic Torrifluvents). The site, located on large and deep alluvial fan, is fairly flat and broadly sloping at $\sim 3.5\%$ from southeast to northwest and minimally dissected by shallow ($< \sim 0.1$ – 0.2 m, nonincised) R channels. These shallow channels are not bordered by the dense woody vegetation lining larger channels of the Santa Rita Experimental Rangeland, suggesting minimal within-channel infiltration at this site. There is one larger (~ 2 – 5 m wide) wash running past the site about ~ 150 m to the northeast and

essentially outside of the flux tower source area, because of the distance and the winds rarely come from this direction (Scott, 2010). Water table depths below this site are unknown but estimated to be very deep and beyond the rooting depth of the plants. The two closest wells, located about 5 km to the east of the site, have water table depths exceeding 100 m (M. McClaran, unpublished data, 2018). This depth is not uncommon for valley floor locations in this region (Thiros et al., 2010).

Over the 2004–2016 study period, mean annual P was 349 ± 67 mm (standard deviation) with 26 ± 21 mm in the dry and warm premonsoon (April–June), 221 ± 41 mm in the warm monsoon months (July–September), 25 ± 14 mm in the cooler, late fall months (October–November), and 76 ± 34 mm in the cooler winter (December–March). The dominant growing season occurs mainly in July through September, but a more variable spring growing season also happens around March through May given sufficient cool season P (Scott et al., 2009). In the broader regional context, this site has a similar magnitude and seasonality of hydrometeorologic conditions and ecosystem water and carbon fluxes as other grasslands and shrublands in the northern half of the North American monsoon region (Biederman et al., 2017; Kurc & Small, 2007; Petrie et al., 2015; Scott et al., 2015; Verduzco et al., 2015).

3. Data

P was measured with a tipping bucket rain gauge (TE525, Texas Electronics) with the orifice 1 m above the ground and located in an intercanopy location somewhat shielded from the wind by nearby trees. Next to it, a second tipping bucket gauge was used to check rainfall amounts or fill in missing data. Precipitation undercatch is a well-documented effect when rain gauges are exposed to the wind (Larson & Peck, 1974). At the nearby Walnut Gulch Experimental Watershed, annual undercatch amounts determined by using 1 m above ground gauges and colocated pit gauges indicate a 3–8% undercatch (D. Goodrich, unpublished data, 2018). Accordingly, we assign an uncertainty to P amounts ranging from $1.0P$ to $1.08P$ in the overall site water budget developed later in the paper.

ET was measured using the eddy covariance (EC) technique with measurement details available elsewhere (Scott, 2010). Daily average ET values were calculated by first filling the gaps in the 30-min data. Gaps were filled using 14-day look-up tables of ET and gap-filled, incoming photosynthetically active radiation, averaged over $100\text{-}\mu\text{mol}\cdot\text{m}^{-2}\cdot\text{s}^{-1}$ intervals. Daytime flux source areas (i.e., 90% integrated flux footprint) are ellipsoid in shape and typically extend out to ~ 200 m from the flux tower (Schmid, 1997; Scott, 2010). Common to most EC sites (Wilson et al., 2002), accumulated sums of latent and sensible heat fluxes over the sums of available energy indicate a lack of energy balance “closure” of 89% (mean annual ratio, range 84–98%), possibly indicating that one or both of the turbulent heat fluxes are underestimated. To account for this, some researchers have suggested “forcing closure” by distributing the underestimation to the turbulent heat fluxes equally by dividing the fluxes by the daily closure fraction (Twine et al., 2000). The accuracy of EC ET measurements has been checked by comparing them with ET estimated from watershed water balances (Barr et al., 2012; Scott, 2010) or lysimeters (Perez-Priego et al., 2017), and these studies generally support the conclusion that EC ET is underestimated. However, comparisons at this site and for other dryland shrubland sites generally show that if there is an underestimation, it is probably less than $\sim 10\%$ (Biederman et al., 2018; Scott, 2010). Still, we consider a closure-adjusted ET as an upper bound ($ET/0.89$ or $1.12ET$) on its uncertainty in the water budget and use $1.0ET$ for the lower bound.

R measurements come from flume data from two small headwater watersheds located about 1.5 km east of our study site (Polyakov et al., 2010). Of these watersheds, WS6 (3.1 ha) has the same soil type as the savanna site, and its small watershed area is similar to the ET flux source area (roughly 1–4 ha in extent). However, erosion control check dams installed in WS6 in 2008 had the effect of considerably reducing R. Thus, we estimate R after 2007 using a power law relationship and daily R amounts on WS7 (1.1 ha), a colocated watershed but with a different, less sandy, soil type and R from WS6 for 2004–2007. The function ($y = 1.45x^{0.66}$) predicts WS6 R with a root mean square error of 1.8 mm/day and the coefficient of determination, $R^2 = 0.84$. Runoff, and even run-on (i.e., water flowing overland or in channels that infiltrates as it travels down slope), in the constantly varying source areas of the ET measurements is unlikely to be accurately quantified by R from a spatially fixed watershed due to the unequal distributions of R source areas and channels between the two source areas. To account for this uncertainty, we consider a wide range of R from $0.5R$

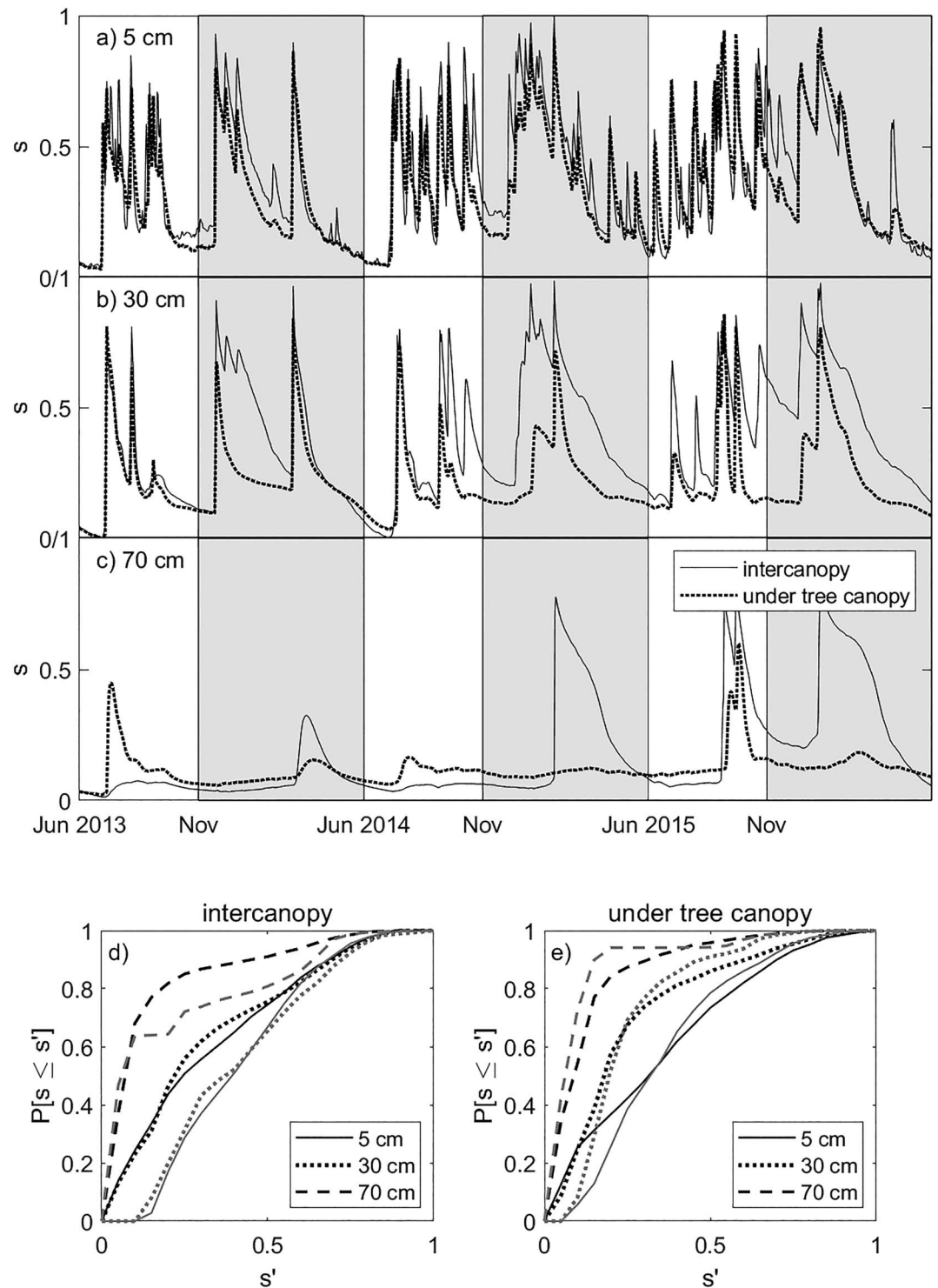


Figure 2. (a–c) Three-hydrologic-year (June 2013 to May 2016) example of time series of soil moisture (relative saturation, s) with winter/spring (November–May) highlighted in gray from intercanopy and under-tree canopy profiles. (d and e) Cumulative probability density functions of 2004–2016 daily soil moisture for different depths (summer months in black; winter in gray), $P[s \leq s']$ represents the probability of s being less than or equal to any value of soil moisture, s' .

to $2.0R$ in the water budget. Considering $R/P = 7\%$ for this study, this uncertainty bounds the range of small watershed R ratios ($R/P = 3\%$ to 14%) measured across the watersheds located on the experimental rangeland (Polyakov et al., 2010).

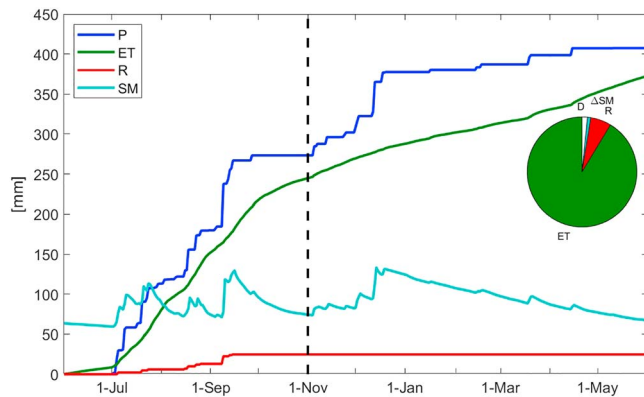


Figure 3. Example of cumulative daily fluxes (precipitation, P, evapotranspiration, ET, and runoff, R) and daily average 0- to 1.3-m root zone soil moisture (SM) at the savanna for the dryland water year running June 2011 through May 2012. Inset pie chart shows proportion of P accounted for by the other water balance components.

Monitored root zone volumetric soil water content (θ , $\text{cm}^3 \text{ water/cm}^3 \text{ soil}$) was measured with probes (CS616, Campbell Scientific) installed at 2.5- to 5-, 5- to 10-, 15- to 20-, 25- to 30-, 45- to 50-, 65- to 70-, 95- to 100-, and 125- to 130-cm depths. One *intercanopy* profile is located about 10 m to the east of the flux tower below bunchgrasses and bare soil between tree canopies, and another *under-tree* profile is located nearby under a large (~5-m-diameter crown) mesquite tree canopy about one half the distance between the tree bole and crown edge. The under-tree profile lacks a probe at the 125- to 130-cm depth. We convert probe output to volumetric SM using a second-order polynomial that was developed in the laboratory using soil from the site. In the lab, three separate probe readings (after reinsertion each time) were made in the watered and hand-mixed soil column for $\theta = 0.0, 0.05, 0.10, 0.15,$ and 0.20 . In the calibration, calculated θ using the polynomial had a root mean square error of 0.011 ($R^2 = 0.97$). The manufacturer's recommendation for temperature compensating the probe output was applied using colocated soil thermocouples.

We use the SM data to develop a number of different metrics. Relative soil saturation (s) is computed as $s = (\theta - \theta_{\min}) / (\theta_{\max} - \theta_{\min})$, where θ_{\min} is the minimum SM and θ_{\max} is the maximum SM at each depth. Total 1.3-m root zone SM for the two locations (SM [mm]) was determined by multiplying θ at each depth by the thickness of each soil layer (75, 75, 100, 150, 200, 250, 300, and 150 mm from shallow to deep) and summing. For the under-tree profile, we assume that θ for the 125- to 130-cm depth was equal to that for the 95- to 100-cm depth. We estimate site-average SM by $0.33SM_{\text{tree}} + 0.67SM_{\text{intercanopy}}$, where 0.33 is the tree canopy fraction. Lastly, we estimate the amount of SM that enters the root zone, SM+, by summing the daily increases in SM: $SM+ = \sum_{i=2}^{n=\text{days}} SM_i - SM_{i-1}$ for $(SM_i - SM_{i-1}) > 0$. This is done using only the intercanopy location to limit the amount of tree canopy rainfall interception. SM+ is used as an estimate of soil water input to compare with seasonal P and ET totals. So long as the soil is not saturated ($\theta = \text{porosity}$), which occurs rarely at this site, SM+ estimates the input of water into the root zone minus some small amount of P that gets intercepted by the grass, litter, or shallow (0–2.5 mm) soil above the first probe depth.

To increase the accuracy of SM measurements, we use a site-specific soil calibration procedure, expected to reduce theta errors (root mean square error) below $\sim 0.04 \text{ m}^3/\text{m}^3$ (Cosh et al., 2016). Our confidence in SM data are increased by results below showing a close, nearly one-to-one linear relationships between seasonal SM+ and ET, as well as for SM+ and P. We do not provide estimates of the SM uncertainty for the long-term water budget, as the net change in SM is very small over the course of the study, and uncertainties due to calibration bias and lack of field scaling are likely minimized when looking at SM differences, which are the key information in the water budget.

Finally, drainage below the monitored root zone, D, is determined as a residual of the other water balance terms using equation (1). The uncertainty in D is calculated by using the range of uncertainty assumed for P, ET, and R (given above) in a combination that either maximizes (highest P, lowest ET, and R) or minimizes D (lowest P, highest ET, and R). This maximization of error approach is conservative in terms of the claimed precision of our water budget.

4. Results

Root zone SM measurements capture the seasonal dynamics of P inputs and ET outputs (Figures 2a–2c show only 3 years for better visualization; see Figure S1 for complete time series). About 63% of the annual average P at this site arrives as convective storms during the summer monsoon months (~July–September), around 22% comes as frontal winter storms (December–March), with the remaining 15% scattered across spring and autumn. While summer storms generate frequent peaks in shallow SM, wetting is generally confined to the upper root zone (0–30 cm) while deeper soil layers remain dry (Figures 2a–2c). Elevated moisture in shallow soil layers is quickly depleted by high evaporative demand and active plants. Greater infiltration is observed in the intercanopy profile that has no tree canopy interception. Comparing total SM increases across the 13-year study, intercanopy SM+ is 34% higher than the

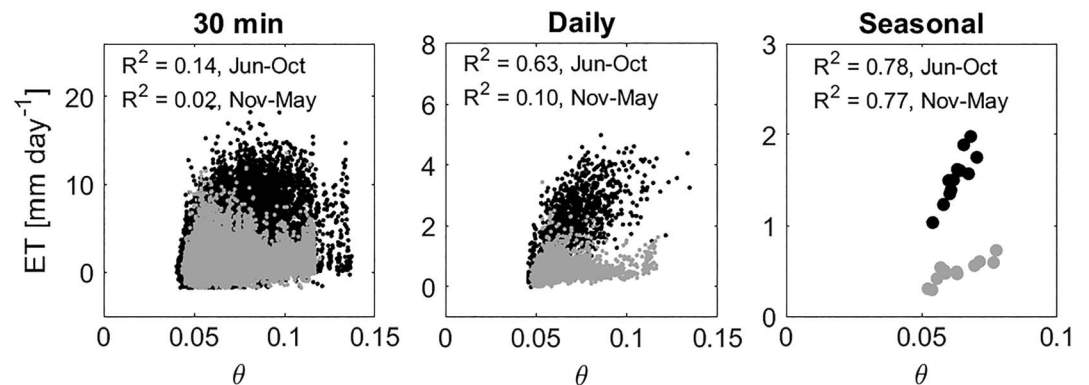


Figure 4. Average 0- to 1.3-m root zone soil moisture (θ , cm^3/cm^3) and evapotranspiration (ET) for June–October (black) and November–May (gray) at half-hourly, daily, and seasonal time scales.

under-tree location, suggesting higher interception losses due to the mature tree canopy and litter layer at this location. Using distributed rain gauges deployed for one summer season under five trees, average tree canopy interception is estimated to be 20%, so the under-tree profile infiltration here may be biased low relative to other locations under trees. For the intercanopy location in winters, infiltration tends to be deeper, and the root zone is wet more often (Figures 2c and 2d) when P intensities are lower, storm durations are longer, and plants are downregulated, resulting in slower drying. The under-tree profile tends to be wetter at the surface in winter but lacks the infiltration to wet the deeper soil layers. We also observe that the wetter summer and winter are bracketed by more consistently dry spring and autumn periods that often result in nearly complete root zone desiccation, especially in the late spring (~May). Thus, in this paper, we use 1 June as a start of the water year to minimize any carryover of the previous season's SM.

A single water year is used to illustrate the seasonal timing and magnitude of fluxes into and out of the critical zone along with the SM state (Figure 3). By the end of the summer/fall season, most of the P becomes ET with a much smaller amount partitioned to R. In the cooler winter season, rainfall increases SM, and ET remains at a small, nearly constant rate (i.e., constant slope of the cumulative flux shown). The rate of decrease in the wintertime SM peak is much slower than the quick dry-down rates seen in summer. ET increases in spring (~April) with rising temperatures and plant upregulation (not shown). By the end of this water year with $P = 407$ mm, ET accounts for 91.3% of P with smaller amounts of R (6.1%), D (1.4%), and net annual change in SM (1.2%). Water year partitioning as a fraction of yearly P across all years ranges from 82%

to 107% for ET, 0% to 15% for R, -5% to 3% for change of SM (ΔSM), and -19% to 11% for D (Figure S2). Only annual P and ET are significantly correlated with each other ($R^2 = 0.79$, $p < 0.001$). Later, we present the cumulative water budget for the entire study period.

While short-term ET rates are regulated by weather, the controls of ET amounts by soil water availability become more obvious with increasing periods of temporal aggregation (Figure 4). Subdaily ET is weakly correlated with SM because of additional controls by the diurnal variation in weather-related energy terms (e.g., radiation, vapor pressure deficit, and temperature). Daily ET is more correlated with θ , because diurnal weather variation is averaged out, although there remains some unaccounted variability due to day-to-day weather. At the seasonal scale, however, variations in year-to-year energy terms are smaller than variations in water availability, and θ accounts for more than 75% of the variation in ET.

Comparing how well ET and P represent seasonal water availability as quantified by SM inputs, we find that seasonal SM+ is closely related to both ET and P (Figure 5, $R^2 \geq 0.83$), but both ET and P usually exceed

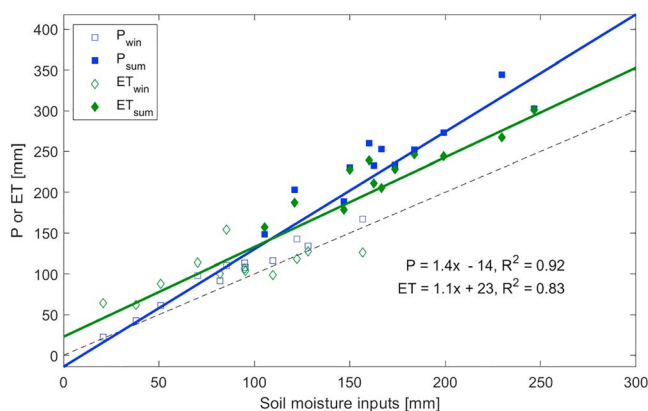


Figure 5. Accumulated winter/spring (November–May) and summer/fall (June–October) soil moisture increases (intercanopy SM+), precipitation (P, blue) and evapotranspiration (ET, green). Regression lines are colored to match symbols that they are fit through, and the dashed line is the 1:1 line.

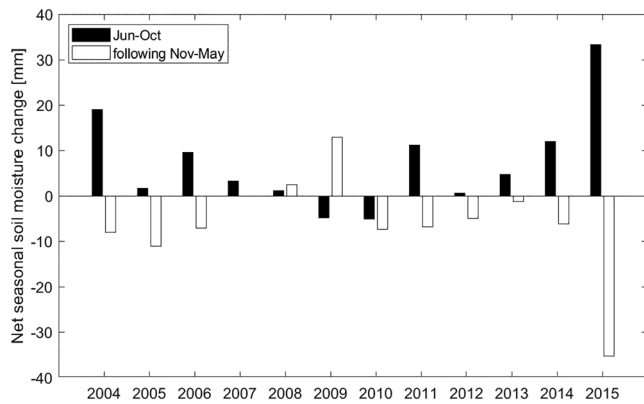


Figure 6. Net seasonal soil moisture changes in the top 1.3 m.

SM+. The line comparing SM+ and ET has a slope near unity but has a positive offset from the 1:1 line. Meanwhile, the slope of the line comparing SM+ and P is steeper than the 1:1 line due to the larger differences in summer/fall, when a greater proportion of P becomes R, reducing the water available to enter the soil and contribute to ET.

During drier winter/springs, ET tends to exceed SM+ more than in wetter cool seasons (Figure 5, open diamonds). In years with wet summers, there may be substantial carryover of SM, which is lost as ET in the following winter/spring period (Figure 6). There is good agreement between increases in SM storage in summer/fall and depletions of storage in winter/spring (root mean square error = 6.7 mm, correlation coefficient = -0.80). Average summer to winter carryover is small, but it is larger in some years (mean = 7.2 mm, range = -5 to +33 mm).

We use the 2015 water year to illustrate the development, evolution, and effects of summer to spring carryover of SM by examining the monthly fluxes and SM storage (2015 had 33 mm of carryover, Figure 6) in the context of the 2004–2014 mean fluxes (Figure 7). The carryover in 2015 is driven by large positive anomalies in late summer P (September–October). While fall ET (September–November) values are accordingly high, SM remains significantly above average at the onset of the cool winter months (December–February) when temperature limits vegetation activity (trees and bunchgrasses are dormant). Above-average P in January adds to the surplus SM, but it is not until later in March and April when this moisture is utilized to support above-average ET. The bunchgrasses can typically start greening in March, while the trees leaf out later in April. More than half of the anomalous winter SM that is not depleted by ET until spring is due to the storage increases from the previous summer.

An additional facet of the moisture carryover is seen in the monthly drainage flux (D, Figure 7). D is higher than average in the wet, late summer period (September–October) due possibly to both root hydraulic descent and direct infiltration, and a significant negative anomaly occurs in the late spring months (April–May). This negative anomaly in D (total of -28 mm for D in April and May) indicates additional storage of the

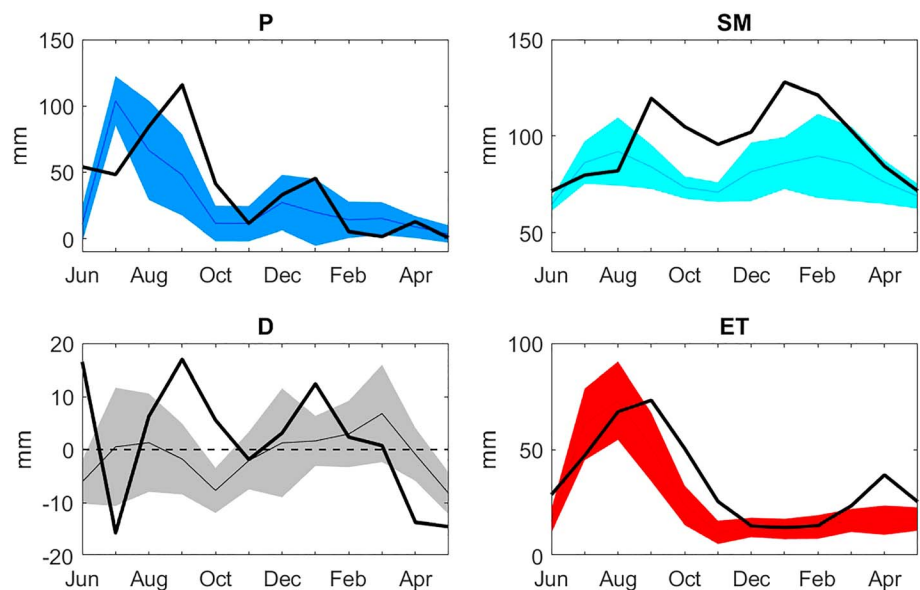


Figure 7. 2015–2016 June–May precipitation (P), 0- to 1.3-m soil moisture (SM), root zone drainage (D, positive is downward) and evapotranspiration (ET). Thicker black lines show 2015–2016 monthly totals (mm), and thin lines with colored envelopes show 2004–2015 monthly means \pm 1 standard deviation.

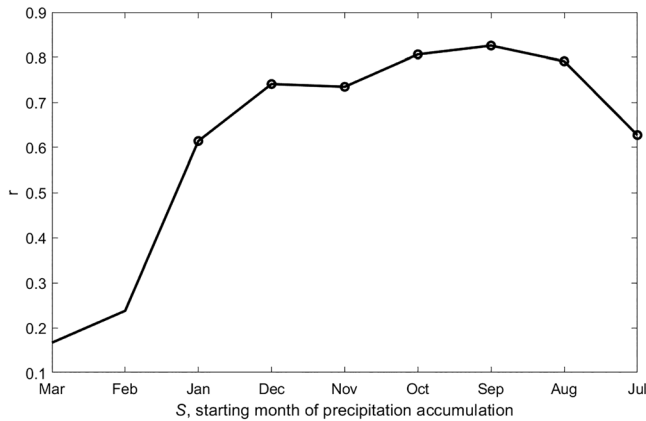


Figure 8. Correlation coefficient (r) between 2004 and 2016 spring growing season evapotranspiration (March–May) and precipitation over the period of month S through May. Significant correlations circled ($p < 0.05$).

abundant late summer rainfall in soil water below the monitored root zone. Moreover, we see additional evidence for the utilization of longer-term storage of antecedent P in the considerable lag in peak correlations between antecedent P and spring seasonal ET totals calculated across the full 13-year record (Figure 8): spring (March–May) ET totals were most correlated with fall–winter–spring (September–May) P .

Over the full 13-year record, the cumulative components of the long-term water balance show the preponderance of ET and its tight coupling with P at this semiarid site (Figure 9a). Estimates of D including systematic uncertainty that brackets the minimum and maximum estimates show that the multiyear movement of water beyond the 0- to 1.3-m root zone (positive D) is likely small (Figure 9b, Table 1). In fact, the uncertainty envelope for estimates of D span mostly negative values, which are not physically plausible for this site with no accessible deep source of moisture. Water table depths at this site are deep ($> \sim 100$ m) and beyond the rooting depth of the plants.

5. Discussion

Our objective is to determine the multiyear critical zone water balance dynamics of a semiarid savanna. Using a unique data set that quantified all water balance fluxes and SM state collected over 13 years, we examine whether expectations about dryland water balance components developed from shorter-duration studies are confirmed over a longer-term period with a wide range of forcing variability and ecosystem functioning. The results support expectations of shallow and flashy SM dynamics and a lack of long-term D below the monitored root zone. We also find a more one-to-one relationship between seasonal water availability, as quantified by SM inputs, and seasonal ET , rather than more commonly used P totals or temporally averaged SM. Finally, we discover unexpected lags in soil water availability and ET , especially when anomalously high summer P carries over and contributes to spring ET . Below we discuss what these results imply for our four expectations about the critical zone water balance in drylands.

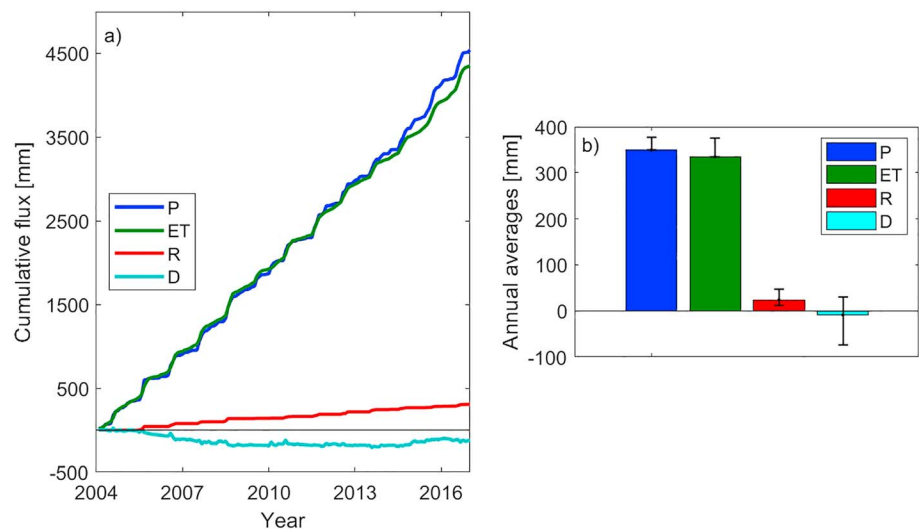


Figure 9. (a) Cumulative water balance terms. (b) Annual averages (2004–2016) with error bars indicating systematic uncertainty: $1.0P - 1.08P$, $1.0ET - 1.12ET$, $0.5R - 2.0R$. $D_{low} = 1.0P - 1.12ET - 2.0R - \Delta SM$. $D_{high} = 1.08P - ET - 0.5R - \Delta SM$. Cumulative change in soil moisture (ΔSM), not shown, is small and fluctuates between ~ -50 mm and 50 mm. P = precipitation; ET = evapotranspiration; R = runoff; D = drainage.

Table 1
Cumulative Root Zone Water Balance Terms With Estimates of Systematic Uncertainty

Total (mm)								
<i>n</i> (days)	P	ET	R	ΔSM	D	%ET of P	%R of P	% D of P
4745	4540	4351	308	1	−121	95.8	6.8	−2.7
Uncertainty +/-								
that make D more +	4903	4351	154	1	397			
that make D more −	4540	4873	617	1	−951			
Average rate (mm/year)								
	P	ET	R	dS	D			
	349	335	24	0	−9			

Note. P uncertainty: $1.0P - 1.08P$ due to gauge undercatch. ET uncertainty: $1.0ET - 1.12ET$. R uncertainty: $0.5R - 2.0R$. ΔSM uncertainty unquantified. P = precipitation; ET = evapotranspiration; R = runoff; D = drainage; ΔSM = change in soil moisture.

1. Soils are infrequently wetted beyond shallow root zone depths (<~30 cm). Deeper, more persistent wetting occurs episodically and mainly in winter when plant activity is limited and evaporative demand is low.

Our data generally support these expectations for SM dynamics, but we find somewhat different patterns between the intercanopy and under-tree locations. However, for both locations, the bulk of the cumulative probability distributions of SM across shallow to deeper depths in the root zone are contained near the dry end, far below the soil's field capacity (Figures 2d and 2e), especially on the dry end at greater depths. This pattern may be explained by the distribution of daily rainfall in this region, where the number of small rainfall days (<~5 mm) is high and larger events are less common (Huxman et al., 2004), even though the larger events largely determine the seasonal and annual totals. Likewise, the bulk of the rainfall comes in the summer, when the plants quickly use this water to support growth and shallow moisture dries quickly (Kurtz & Small, 2007). Thus, abiotic evaporation is a significant part of ET in this region (Cavanaugh et al., 2011; Scott & Biederman, 2017).

We also find that the intercanopy position has less interception of P and deeper infiltration (Figure 2). The deeper soil wetting tends to occur more episodically, mainly in wet fall and winter periods when evaporative demand is lower and plant activity is limited by lower temperatures. High evaporative demand in summer and opportunistic dryland vegetation impose a strong constraint on deep infiltration, because ET quickly uses any available SM (Andraski, 1997; Scanlon et al., 2005; Scott et al., 2000). Furthermore, this vegetation constraint is compounded by deeper-rooted dryland shrubs or trees that severely restrict the possibility of deep D beyond the root zone and, ultimately, of recharge (Collins & Bras, 2007; Keese et al., 2005).

These findings about SM dynamics should be considered in light of the relatively high degree of uncertainty in their spatial representativeness across the site (Cosh et al., 2016; Templeton et al., 2014). However, the simple planar topography of the site, the high infiltration capacity of the loamy sand soils, and the lack of clearly defined R channels limit the possibility of regions of enhanced infiltration due to topography. Thus, spatial variability in SM is mainly related to vegetation cover at this site, and we account for this variability (albeit to a limited degree) by using the intercanopy and under-tree profiles used to quantify SM. The uncertainty in the SM measurements is further tempered by using them to quantify the ΔSM, which is small over longer integration times in the water budget (e.g., Figures 3 and 9).

2. Seasonal water availability, estimated by SM inputs, is best quantified by ET rather than the commonly used, time-averaged SM or P

While diurnal and daily variability in weather-related energy terms control short-term ET rates, longer-term integrated ET is directly related to water supply, that is, SM, which limits the amount that can evaporate from the soil or be used by plants. Correlations between root zone SM and ET substantially increase from subdaily to seasonal periods (Figure 4). However, we see smaller amounts of seasonal ET for a given average moisture content for the winter/spring (November–May) than the main growing season (June–October, Figure 4c). This is because the temporally averaged SM state does not indicate the amount of available water. Instead, the longer persistence of soil water in winter leads to higher averages. Therefore, it is the SM inputs,

SM+, which consistently predict seasonal ET, rather than the average SM state (Figure 5). Over shorter averaging times, additional regulation by varying evaporative demand (i.e., weather) obscures the SM link. Thus, studies using shorter-term data in dryland regions have examined the SM controls on ET by normalizing ET by potential ET (ET_p). This typically results in a function for ET/ET_p that increases linearly with SM below some threshold (stage II ET) and saturates to a constant value thereafter (e.g. Kurc & Small, 2004, Vivoni et al., 2008). Beyond this threshold, moisture is no longer limiting ET (stage I ET). However, at dryland sites such as in this study, this condition is rare, especially during the growing season, such that at seasonal time scales we do not find saturating conditions.

Next, we confirm a direct link of seasonal sums of ET (slope close to 1 with small y-axis offset), rather than P, with root zone water inputs (Figure 5). At our site, the R ratio, R/P , averages 8.9% in summer and 0.9% in winter, so the seasonal difference contributes to the considerable 1.5 slope of P with SM+ (Figure 5). Many ecohydrological studies use P as a metric of water availability in absence of SM data, but R can be a significant fraction of P (Biederman et al., 2018; Polyakov et al., 2010), so using P as a water availability metric that drives productivity can complicate interpretation (Ponce-Campos et al., 2013). Biederman et al. (2018) suggest that this is because over seasonal to annual time scales, ET quantifies the amount of P partitioned to recharge SM. They also show some support for this linkage with a closer agreement between ET and the difference $P - R$ than for ET and P alone. Our study substantiates the direct relationship between the amount of water that enters the soil and the subsequent efflux of that water back to the atmosphere.

Seasonal totals of ET and P are usually greater than SM+ (Figure 5). We expect that some amount of P is either intercepted before entering the soil or only wets the shallow surface soil (0–2.5 cm) and is not detected by the SM measurements. For example, summers average 24 rainfall events with depths of 0–5 mm that total 35 mm. Winters average 15 days of these small events with a total of 22 mm. These totals are reasonably close to the average ET and SM+ differences (54 mm in summer and 15 mm in winter), supporting the idea that most of the water in such small rainfall events is lost to surface evaporation/interception.

The close agreement between SM+ and measured ET without any adjustments for lack of energy balance closure also suggests that the eddy flux measurements of ET quantify the water vapor efflux quite accurately at this site (Figure 5). The long-term water budget provides additional support that any sort of closure adjustment like that of Twine et al. (2000) is probably not warranted. This finding is supported by data collected at other dryland sites, where there is often close agreement between P minus R and ET (Biederman et al., 2018; Scott, 2010). Moreover, the good agreement between SM+ and ET as well as between SM+ and P suggests that there is good spatial representativeness of SM from using just this one intercanopy profile.

3. Precipitation stored as SM is reliably depleted within the current (i.e., spring or summer) growing season. Therefore, seasonal ET should be constrained by within-season SM inputs.

Contrary to this expectation, we find evidence for episodic summer to spring carryover of SM. Drier winters ($P < \sim 100$ mm) have ET totals that generally exceed P (Figure 5, open diamonds), and some winters (e.g., 2015) have substantial carryover of SM from the summer/fall period (Figure 6). This carryover of episodic summer moisture excesses and subsequent use of it by the end of the following spring suggests that for this climate, 1 June is a more appropriate start to a hydrologic water year than traditionally used fall starting dates. The predictably dry and hot spring period (April–June) consistently exhausts all available SM.

While carryover of significant amounts of summer SM is rare (Figure 6), we see that ET can be impacted all the way to the start of the next summer growing season (Figures 7 and 8). In late 2015, anomalously high SM results in high ET through the late summer/fall (September–November), but the coldest period of winter (December–February) shuts down ET and leaves elevated amounts of moisture in the soil until the plants (grasses and trees) could upregulate in spring, resulting in higher than average ET throughout this season. This high springtime ET in 2016 is associated with unusually high levels of plant photosynthesis as well (Smith et al., 2018). Additional evidence of ecosystem memory of antecedent P is seen with a considerable lag in peak correlations between antecedent P amounts and spring seasonal ET totals (Figure 8). March–May ET totals are most correlated with September–May P. Consistent with climate model forecasts (McAfee & Russell, 2008), winter/spring P has substantially declined in the 21st century for this region (Scott et al., 2015). These declines have led to reductions in plant cover, especially grasses (Bodner &

Robles, 2017). While climate models are inconsistent in forecasted summer/fall P amounts in this region, increased warm-season P could possibly bolster winter decreases through winter SM carryover.

Even though SM dynamics are shallow, monthly D below the 1.3-m monitoring depth (D) could be positive or negative (Figure 7). For example in 2015, an anomalously wet June and late summer results in positive D, and a drier-than-average July and the following normally dry spring had negative amounts, implying additional SM carryover deep in the soil. D can be positive due to both direct infiltration beyond 1.3-m depth and hydraulic descent (i.e., downward HR) by plant roots. Lee et al. (2018), with sap flow measurements in tap roots and modeling, confirm these patterns of hydraulic descent and subsequent tree water use, as well as the preponderance of hydraulic descent (deep SM increases) for the June through December 2015 period. Unfortunately, their study ended before the following 2016 spring growing season and cannot be used to independently evaluate the results here: abundant water use from the monitored root zone and below indicated by decreases in SM and negative D (Figure 7). Thus, HR is likely facilitating seasonal carryover of SM (Fu et al., 2016).

4. Long-term D is expected to be near zero, resulting in negligible groundwater recharge.

Our analysis provides strong support of this expectation. Without considering any systematic uncertainty in the fluxes, ET is the dominant efflux (96%) of incoming P inputs. R is much smaller (7%), and D is even smaller (−3%). When considering uncertainties (to bracket the underestimation of P due to gauge undercatch, the possible underestimation of ET due to a lack of energy balance closure at this site, and the overestimation or underestimation of R within the source area of the ET flux measured by the tower), D from the monitored root zone was estimated to be as large as 31 mm/year (9% of annual P) and as small as −73 mm/year (−21% of P) over the 13-year study period. Thus, long-term net D is indistinguishable from zero. While our water balance approach does not directly measure that long-term D is small, numerous studies using soil chloride accumulations under root zones support the fact that negligible D below root zone is occurring under these upland, valley locations (Coes & Pool, 2007; Scanlon et al., 2006; Seyfried et al., 2005; Walvoord et al., 2002). Additional support comes from shorter-term watershed or lysimeter studies showing that opportunistic dryland vegetation can quickly and completely extract SM when available (Scanlon et al., 2005; Scott, 2010).

Given the focus of this study on one site, it is important to discuss how long-term drainage/recharge may vary across the dryland landscape of the Southwest. There are a number of site factors that might be limiting D at our site. The topography is planar and gently sloping with a nonincised, poorly defined channel network. This limits the concentration of R into channels and subsequent transmission losses. Furthermore, the deep loamy sands at the site favor infiltration and limit overland flow (Polyakov et al., 2010). However, we find that the infiltrated water is thoroughly used by ET (Figure 5) limiting deeper root zone wetting (Figure 2). Also, the deeply rooted trees appear to be capable of accessing this moisture, even below the 1.3-m depth of monitoring, as indicated by negative D amounts in seasonal (Figure 7) and annual totals (Figure S2). While these site factors may be serving to make D small, many other studies across the drylands of the Southwest echo these results.

In contrast to these results showing often-negligible recharge in upland locations, studies of large ephemeral channels (draining large areas, $\sim 10^4$ – 10^5 ha) have shown that considerable amounts of R can infiltrate in them and recharge basin groundwater (Blasch et al., 2006; Coes & Pool, 2007; Goodrich et al., 2004; Pool, 2005). Considering the possibility of recharge occurring in smaller channels with less R and transmission losses, it is often unknown how much of channel infiltration is subsequently extracted by denser, deep-rooted shrubs and trees lining ephemeral channels, indicating enhanced water availability (Stromberg et al., 2017). One study from an upland shrub site in New Mexico, using measurements and equation (1), estimated that D was large and ultimately becomes groundwater recharge (26% of the site's 238-mm mean annual P) due to small channel infiltration (Schreiner-McGraw & Vivoni, 2017). However, we note the difficulty of using a water balance approach to estimate recharge within a small watershed because of the following: (1) EC and SM measurements may not be representative of the same distribution of upland and channel areas; (2) there can be a similar, if not greater, mismatch in source areas for the ET measurements and where the focused channel infiltration occurs; and (3) D is calculated as the residual of larger fluxes, the uncertainty of which may exceed the magnitude of D. We recommend additional studies with measurements specifically focused on the amount and fate of in-channel R losses and their role in site-to-region dryland water balance.

6. Conclusions

Determining how P is partitioned within the critical zone is one of the most fundamental challenges in hydrology. This paper quantifies the terms of the critical zone water balance over a 13-year period in a semi-arid upland savanna in the American Southwest. Our results confirm that SM dynamics are highly variable and usually confined to the upper root zone. Deeper root zone wetting happens infrequently and is aided by decreases in evaporative demand and plant root water uptake. Seasonal ET is closely related to average root zone SM and closely matches SM inputs. Contrary to expectations, we find that wet summers can result in moisture storage within and below the root zone lasting through winter and supplying moisture for spring-time ET. ET dominates the water loss from the critical zone, R is small, and permanent/net deep D is indistinguishable from zero.

Acknowledgments

Funding for the continued operation of this AmeriFlux site, US-SRM, comes from the USDA Agricultural Research Service and U.S. Department of Energy's Office of Science. The data and analysis codes for the figures and tables in this study are available upon request from the corresponding author. Alternatively, data for this study are available at <http://ameriflux.lbl.gov>, and runoff data are available at <https://www.tucson.ars.ag.gov/dap/>. USDA is an equal opportunity employer.

References

- Adams, D. K., & Comrie, A. C. (1997). The North American monsoon. *Bulletin of the American Meteorological Society*, 78(10), 2197–2213. [https://doi.org/10.1175/1520-0477\(1997\)078<2197:TNAM>2.0.CO;2](https://doi.org/10.1175/1520-0477(1997)078<2197:TNAM>2.0.CO;2)
- Ajami, H., Troch, P. A., Maddock, T., Meixner, T., & Eastoe, C. (2011). Quantifying mountain block recharge by means of catchment-scale storage-discharge relationships. *Water Resources Research*, 47, W04504. <https://doi.org/10.1029/2010WR009598>
- Andraski, B. J. (1997). Soil-water movement under natural-site and waste-site conditions: A multiple-year field study in the Mojave Desert, Nevada. *Water Resources Research*, 33(8), 1901–1916.
- Barr, A. G., van der Kamp, G., Black, T. A., McCaughey, J. H., & Nescic, Z. (2012). Energy balance closure at the BERMS flux towers in relation to the water balance of the White Gull Creek watershed 1999–2009. *Agricultural and Forest Meteorology*, 153, 3–13.
- Barron-Gafford, G. A., Sanchez-Cañete, E. P., Minor, R. L., Hendryx, S. M., Lee, E., Sutter, L. F., et al. (2017). Impacts of hydraulic redistribution on grass–tree competition vs facilitation in a semi-arid savanna. *The New Phytologist*, 215(4), 1451–1461. <https://doi.org/10.1111/nph.14693>
- Biederman, J. A., Scott, R. L., Arnore Iii, J. A., Jasoni, R. L., Litvak, M. E., Moreo, M. T., et al. (2018). Shrubland carbon sink depends upon winter water availability in the warm deserts of North America. *Agricultural and Forest Meteorology*, 249, 407–419. <https://doi.org/10.1016/j.agrformet.2017.11.005>
- Biederman, J. A., Scott, R. L., Bell, T. W., Bowling, D. R., Dore, S., Garatuza-Payan, J., et al. (2017). CO₂ exchange and evapotranspiration across dryland ecosystems of southwestern North America. *Global Change Biology*, 23(10), 4204–4221. <https://doi.org/10.1111/gcb.13686>
- Biederman, J. A., Scott, R. L., Goulden, M. L., Vargas, R., Litvak, M. E., Kolb, T. E., et al. (2016). Terrestrial carbon balance in a drier world: The effects of water availability in southwestern North America. *Global Change Biology*, 22(5), 1867–1879. <https://doi.org/10.1111/gcb.13222>
- Blasch, K. W., Ferré, T., Hoffmann, J. P., & Fleming, J. B. (2006). Relative contributions of transient and steady state infiltration during ephemeral streamflow. *Water Resources Research*, 42, W08405. <https://doi.org/10.1029/2005WR004049>
- Bodner, G. S., & Robles, M. D. (2017). Enduring a decade of drought: Patterns and drivers of vegetation change in a semi-arid grassland. *Journal of Arid Environments*, 136, 1–14. <https://doi.org/10.1016/j.jaridenv.2016.09.002>
- Brooks, P. D., Chorover, J., Fan, Y., Godsey, S. E., Maxwell, R. M., McNamara, J. P., & Tague, C. (2015). Hydrological partitioning in the critical zone: Recent advances and opportunities for developing transferable understanding of water cycle dynamics. *Water Resources Research*, 51, 6973–6987. <https://doi.org/10.1002/2015WR017039>
- Burgess, S. S. O., Adams, M. A., Turner, N. C., & Ong, C. K. (1998). The redistribution of soil water by tree root systems. *Oecologia*, 115(3), 306–311. <https://doi.org/10.1007/s004420050521>
- Caldwell, M. M., Dawson, T. E., & Richards, J. H. (1998). Hydraulic lift: Consequences of water efflux from the roots of plants. *Oecologia*, 113(2), 151–161. <https://doi.org/10.1007/s004420050363>
- Cavanaugh, M. L., Kurc, S. A., & Scott, R. L. (2011). Evapotranspiration partitioning in semiarid shrubland ecosystems: A two-site evaluation of soil moisture control on transpiration. *Ecohydrology*, 4(5), 671–681. <https://doi.org/10.1002/eco.157>
- Coes, A. L., & Pool, D. R. (2007). Ephemeral-stream channel and basin-floor infiltration and recharge in the Sierra Vista Subwatershed of the Upper San Pedro Basin, southeastern Arizona, Report Rep. 1703J.
- Collins, D., & Bras, R. (2007). Plant rooting strategies in water-limited ecosystems. *Water Resources Research*, 43, W06407. <https://doi.org/10.1029/2006WR005541>
- Cosh, M. H., Ochsner, T. E., McKee, L., Dong, J., Basara, J. B., Evett, S. R., et al. (2016). The soil moisture active passive Marena, Oklahoma, in situ sensor testbed (smap-moisst): Testbed design and evaluation of in situ sensors. *Vadose Zone Journal*, 15(4). <https://doi.org/10.2136/vzj2015.09.0122>
- Dingman, S. (2002). Water in soils: Infiltration and redistribution. *Physical hydrology* (Chap. 6, pp. 220–269). Upper Saddle River, NJ: Prentice-Hall, Inc.
- Fu, C., Wang, G., Goulden, M. L., Scott, R. L., Bible, K., & Cardon, Z. G. (2016). Combined measurement and modeling of the hydrological impact of hydraulic redistribution using CLM4.5 at eight AmeriFlux sites. *Hydrology and Earth System Sciences*, 20(5), 2001–2018. <https://doi.org/10.5194/hess-20-2001-2016>
- Goodrich, D. C., Lane, L. J., Shillito, R. M., Miller, S. N., Syed, K. H., & Woolhiser, D. A. (1997). Linearity of basin response as a function of scale in a semiarid watershed. *Water Resources Research*, 33(12), 2951–2965. <https://doi.org/10.1029/97WR01422>
- Goodrich, D. C., Williams, D. G., Unkrich, C. L., Hogan, J. F., Scott, R. L., Hultine, K. R., et al. (2004). Comparison of methods to estimate ephemeral channel recharge, Walnut Gulch, San Pedro River basin, Arizona. In J. F. Hogan, F. M. Phillips, & B. R. Scanlon (Eds.), *Groundwater recharge in a desert environment: The southwestern United States, Water Resources and Application Series* (Vol. 9, pp. 77–99). Washington, DC: American Geophysical Union.
- Hultine, K. R., Scott, R. L., Cable, W. L., Goodrich, D. C., & Williams, D. G. (2004). Hydraulic redistribution by a dominant, warm-desert phreatophyte: Seasonal patterns and response to precipitation pulses. *Functional Ecology*, 18(4), 530–538. <https://doi.org/10.1111/j.0269-8463.2004.00867.x>
- Huxman, T. E., Snyder, K. A., Tissue, D., Leffler, A. J., Ogle, K., Pockman, W. T., et al. (2004). Precipitation pulses and carbon fluxes in semiarid and arid ecosystems. *Oecologia*, 141(2), 254–268. <https://doi.org/10.1007/s00442-004-1682-4>

- Keese, K., Scanlon, B., & Reedy, R. (2005). Assessing controls on diffuse groundwater recharge using unsaturated flow modeling. *Water Resources Research*, *41*, W06010. <https://doi.org/10.1029/2004WR003841>
- Knapp, A. K., Hoover, D. L., Wilcox, K. R., Avolio, M. L., Koerner, S. E., La Pierre, K. J., et al. (2015). Characterizing differences in precipitation regimes of extreme wet and dry years: Implications for climate change experiments. *Global Change Biology*, *21*(7), 2624–2633. <https://doi.org/10.1111/gcb.12888>
- Kurc, S. A., & Small, E. E. (2004). Dynamics of evapotranspiration in semiarid grassland and shrubland ecosystems during the summer monsoon season, central New Mexico. *Water Resources Research*, *40*, W09305. <https://doi.org/10.1029/2004WR003068>
- Kurc, S. A., & Small, E. E. (2007). Soil moisture variations and ecosystem-scale fluxes of water and carbon in semiarid grassland and shrubland. *Water Resources Research*, *43*, W06416. <https://doi.org/10.1029/2006WR005011>
- Larson, L. W., & Peck, E. L. (1974). Accuracy of precipitation measurements for hydro-logic modeling. *Water Resources Research*, *10*, 857–863. <https://doi.org/10.1029/WR010i004p00857>
- Lee, E., Kumar, P., Barron-Gafford, G. A., Hendryx, S., Sanchez-Cañete, E. P., Minor, R., et al. (2018). Impact of hydraulic redistribution on multispecies vegetation water use in a semiarid savanna ecosystem: An experimental and modeling synthesis. *Water Resources Research*, *54*, 4009–4027. <https://doi.org/10.1029/2017WR021006>
- McAfee, S. A., & Russell, J. L. (2008). Impact of the Northern Annular Mode on cool season climate patterns in the Southwest. *Geophysical Research Letters*, *35*, L17701. <https://doi.org/10.1029/2008GL034828>
- McClaran, M. P. (2003). A century of vegetation change on the Santa Rita Experimental Range. In M. P. McClaran, P. F. Ffolliott, & C. B. Edminster (Eds.), *Santa Rita Experimental Range: One-hundred years (1903–2003) of accomplishments and contributions* (pp. 16–33). Ogden, UT: USDA Forest Service, Rocky Mountain Research Station.
- Nadezhkina, N., David, T. S., David, J. S., Ferreira, M. I., Dohnal, M., Tesář, M., et al. (2010). Trees never rest: The multiple facets of hydraulic redistribution. *Ecohydrology*, *3*(4), 431–444. <https://doi.org/10.1002/eco.148>
- Newman, B. D., Wilcox, B. P., Archer, S. R., Breshears, D. D., Dahm, C. N., Duffy, C. J., et al. (2006). Ecohydrology of water-limited environments: A scientific vision. *Water Resources Research*, *42*, W06302. <https://doi.org/10.1029/2005WR004141>
- Nicholson, S. E. (2011). *Dryland climatology*. Cambridge, UK: Cambridge University Press. <https://doi.org/10.1017/CBO9780511973840>
- Novick, K. A., Ficklin, D. L., Stoy, P. C., Williams, C. A., Bohrer, G., Oishi, A. C., et al. (2016). The increasing importance of atmospheric demand for ecosystem water and carbon fluxes. *Nature Climate Change*, *6*(11), 1023–1027. <https://doi.org/10.1038/nclimate3114>
- Noy-Meir, I. (1973). Desert ecosystems: Environment and producers. *Annual Review of Ecology and Systematics*, *4*(1), 25–51. <https://doi.org/10.1146/annurev.es.04.110173.000325>
- Perez-Priego, O., El-Madany, T. S., Migliavacca, M., Kowalski, A. S., Jung, M., Carrara, A., et al. (2017). Evaluation of eddy covariance latent heat fluxes with independent lysimeter and sapflow estimates in a Mediterranean savannah ecosystem. *Agricultural and Forest Meteorology*, *236*, 87–99. <https://doi.org/10.1016/j.agrformet.2017.01.009>
- Petrie, M., Collins, S., Swann, A., Ford, P., & Litvak, M. (2015). Grassland to shrubland state transitions enhance carbon sequestration in the northern Chihuahuan Desert. *Global Change Biology*, *21*(3), 1226–1235. <https://doi.org/10.1111/gcb.12743>
- Polyakov, V. O., Nearing, M. A., Nichols, M. H., Scott, R. L., Stone, J. J., & McClaran, M. P. (2010). Long-term runoff and sediment yields from small semiarid watersheds in southern Arizona. *Water Resources Research*, *46*, W09512. <https://doi.org/10.1029/2009WR009001>
- Ponce-Campos, G. E., Moran, M. S., Huete, A., Zhang, Y., Bresloff, C., Huxman, T. E., et al. (2013). Ecosystem resilience despite large-scale altered hydroclimatic conditions. *Nature*, *494*(7437), 349–352. <https://doi.org/10.1038/nature11836>
- Pool, D. (2005). Variations in climate and ephemeral channel recharge in southeastern Arizona, United States. *Water Resources Research*, *41*, W11403. <https://doi.org/10.1029/2004WR003255>
- Reynolds, J. F., Kemp, P. R., Ogle, K., & Fernández, R. J. (2004). Modifying the ‘pulse-reserve’ paradigm for deserts of North America: Precipitation pulses, soil water, and plant responses. *Oecologia*, *141*(2), 194–210. <https://doi.org/10.1007/s00442-004-1524-4>
- Rodríguez-Iturbe, I. (2000). Ecohydrology: A hydrologic perspective of climate-soil-vegetation dynamics. *Water Resources Research*, *36*(1), 3–9. <https://doi.org/10.1029/1999WR900210>
- Sandvíg, R. M., & Phillips, F. M. (2006). Ecohydrological controls on soil moisture fluxes in arid to semiarid vadose zones. *Water Resources Research*, *42*, W08422. <https://doi.org/10.1029/2005WR004644>
- Scanlon, B. R., Keese, K. E., Flint, A. L., Flint, L. E., Gaye, C. B., Edmunds, W. M., & Simmers, I. (2006). Global synthesis of groundwater recharge in semiarid and arid regions. *Hydrological Processes*, *20*(15), 3335–3370. <https://doi.org/10.1002/hyp.6335>
- Scanlon, B. R., Langford, R. P., & Goldsmith, R. S. (1999). Relationship between geomorphic settings and unsaturated flow in an arid setting. *Water Resources Research*, *35*(4), 983–999. <https://doi.org/10.1029/98WR02769>
- Scanlon, B. R., Levitt, D. G., Reedy, R. C., Keese, K. E., & Sully, M. J. (2005). Ecological controls on water-cycle response to climate variability in deserts. *Proceedings of the National Academy of Sciences of the United States of America*, *102*(17), 6033–6038. <https://doi.org/10.1073/pnas.0408571102>
- Schmid, H. P. (1997). Experimental design for flux measurements: Matching scales of observations and fluxes. *Agricultural and Forest Meteorology*, *87*(2–3), 179–200. [https://doi.org/10.1016/S0168-1923\(97\)00011-7](https://doi.org/10.1016/S0168-1923(97)00011-7)
- Schreiner-McGraw, A. P., & Vivoni, E. R. (2017). Percolation observations in an arid piedmont watershed and linkages to historical conditions in the Chihuahuan Desert. *Ecosphere*, *8*(11). <https://doi.org/10.1002/ecs2.2000>
- Scott, R. L. (2010). Using watershed water balance to evaluate the accuracy of eddy covariance evaporation measurements for three semiarid ecosystems. *Agricultural and Forest Meteorology*, *150*(2), 219–225. <https://doi.org/10.1016/j.agrformet.2009.11.002>
- Scott, R. L., & Biederman, J. A. (2017). Partitioning evapotranspiration using long-term carbon dioxide and water vapor fluxes. *Geophysical Research Letters*, *44*, 6833–6840. <https://doi.org/10.1002/2017GL074324>
- Scott, R. L., Biederman, J. A., Hamerlynck, E. P., & Barron-Gafford, G. A. (2015). The carbon balance pivot point of southwestern U.S. semiarid ecosystems: Insights from the 21st century drought. *Journal of Geophysical Research: Biogeosciences*, *120*, 2612–2624. <https://doi.org/10.1002/2015JG003181>
- Scott, R. L., Cable, W. L., & Hultine, K. R. (2008). The ecohydrologic significance of hydraulic redistribution in a semiarid savanna. *Water Resources Research*, *44*, W02440. <https://doi.org/10.1029/2007WR006149>
- Scott, R. L., Hamerlynck, E. P., Jenerette, G. D., Moran, M. S., & Barron-Gafford, G. A. (2010). Carbon dioxide exchange in a semidesert grassland through drought-induced vegetation change. *Journal of Geophysical Research*, *115*, G03026. <https://doi.org/10.1029/2010JG001348>
- Scott, R. L., Jenerette, G. D., Potts, D. L., & Huxman, T. E. (2009). Effects of seasonal drought on net carbon dioxide exchange from a woody-plant-encroached semiarid grassland. *Journal of Geophysical Research*, *114*, G04004. <https://doi.org/10.1029/2008JG000900>
- Scott, R. L., Shuttleworth, W. J., Keefer, T. O., & Warrick, A. W. (2000). Modeling multiyear observations of soil moisture recharge in the semiarid American Southwest. *Water Resources Research*, *36*(8), 2233–2247. <https://doi.org/10.1029/2000WR900116>

- Seyfried, M. S., Schwinning, S., Walvoord, M. A., Pockman, W. T., Newman, B. D., Jackson, R. B., & Phillips, F. M. (2005). Ecohydrological control of deep drainage in arid and semiarid regions. *Ecology*, *86*(2), 277–287. <https://doi.org/10.1890/03-0568>
- Smith, W. K., Biederman, J. A., Scott, R. L., Moore, D. J. P., He, M., Kimball, J. S., et al. (2018). Chlorophyll fluorescence better captures seasonal and interannual gross primary productivity dynamics across dryland ecosystems of southwestern North America. *Geophysical Research Letters*, *45*, 748–757. <https://doi.org/10.1002/2017GL075922>
- Stromberg, J. C., Setaro, D. L., Gallo, E. L., Lohse, K. A., & Meixner, T. (2017). Riparian vegetation of ephemeral streams. *Journal of Arid Environments*, *138*, 27–37. <https://doi.org/10.1016/j.jaridenv.2016.12.004>
- Templeton, R. C., Vivoni, E. R., Méndez-Barroso, L. A., Pierini, N. A., Anderson, C. A., Rango, A., et al. (2014). High-resolution characterization of a semiarid watershed: Implications on evapotranspiration estimates. *Journal of Hydrology*, *509*(0), 306–319. <https://doi.org/10.1016/j.jhydrol.2013.11.047>
- Thiros, S. A., Bexfield, L. M., Anning, & Huntington, J. M. (2010). Conceptual understanding and groundwater quality of selected basin-fill aquifers in the southwestern United States Rep. 2330-7102, U.S. Geological Survey.
- Twine, T. E., Kustas, W. P., Norman, J. M., Cook, D. R., Houser, P. R., Meyers, T. P., et al. (2000). Correcting eddy-covariance flux underestimates over a grassland. *Agricultural and Forest Meteorology*, *103*(3), 279–300. [https://doi.org/10.1016/S0168-1923\(00\)00123-4](https://doi.org/10.1016/S0168-1923(00)00123-4)
- Verduzco, V. S., Garatuzza-Payán, J., Yépez, E. A., Watts, C. J., Rodríguez, J. C., Robles-Morua, A., & Vivoni, E. R. (2015). Variations of net ecosystem production due to seasonal precipitation differences in a tropical dry forest of northwest Mexico. *Journal of Geophysical Research: Biogeosciences*, *120*, 2081–2094. <https://doi.org/10.1002/2015JG003119>
- Vivoni, E. R., Moreno, H. A., Mascaro, G., Rodríguez, J. C., Watts, C. J., Garatuzza-Payan, J., & Scott, R. L. (2008). Observed relation between evapotranspiration and soil moisture in the North American monsoon region. *Geophysical Research Letters*, *35*, L22403. <https://doi.org/10.1029/2008GL036001>
- Walvoord, M. A., Plummer, M. A., Phillips, F. M., & Wolfsberg, A. V. (2002). Deep arid system hydrodynamics 1. Equilibrium states and response times in thick desert vadose zones. *Water Resources Research*, *38*(12), 1308. <https://doi.org/10.1029/2001WR000824>
- Wilson, J. L., & Guan, H. (2004). Mountain-block hydrology and mountain-front recharge. In *Groundwater recharge in a desert environment: The southwestern United States* (Vol. 9, pp. 113–137). Washington, DC: American Geophysical Union.
- Wilson, K., Goldstein, A., Falge, E., Aubinet, M., Baldocchi, D., Berbigier, P., et al. (2002). Energy balance closure at FLUXNET sites. *Agricultural and Forest Meteorology*, *113*(1–4), 223–243. [https://doi.org/10.1016/S0168-1923\(02\)00109-0](https://doi.org/10.1016/S0168-1923(02)00109-0)